ACS APPLIED MATERIALS & INTERFACES

Review

www.acsami.org

Quantum-Dot-Based Photoelectrochemical Sensors for Chemical and Biological Detection

Zhao Yue,[†] Fred Lisdat,[⊥] Wolfgang J. Parak,[‡] Stephen G. Hickey,[§] Liping Tu,[†] Nadeem Sabir,[‡] Dirk Dorfs,[#] and Nadja C. Bigall[‡,#,*]

[†]Department of Electronics, Nankai University, Tianjin 300071, P.R. China

[‡]Fachbereich Physik und WZMW, Philipps Universität Marburg, Marburg, Germany

[§]Physikalische Chemie/Elektrochemie, Technische Universität Dresden, 01069 Dresden, Germany

[⊥]Biosystems Technology, Technical University of Applied Sciences, Wildau, Germany

[#]Physical Chemistry and Electrochemistry, Leibniz University of Hannover, 30167 Hannover, Germany

ABSTRACT: Quantum-dot-based photoelectrochemical sensors are powerful alternatives for the detection of chemicals and biochemical molecules compared to other sensor types, which is the primary reason as to why they have become a hot topic in nanotechnology-related analytical methods. These sensors basically consist of QDs immobilized by a linking molecule (linker) to an electrode, so that upon their illumination, a photocurrent is generated which depends on the type and concentration of the respective analyte in the immediate environment of the electrode. The present review provides an overview of recent developments in the fabrication methods and sensing concepts concerning direct and indirect interactions of the analyte with quantum dot modified electrodes. Furthermore, it describes in detail the broad range of different sensing applications of such quantum-dot-based photoelectrochemical sensors for inorganic and organic (small and macro-) molecules that have arisen in recent years. Finally, a number of aspects concerning current challenges on the way to achieving real-life applications of QD-based photochemical sensing are addressed.

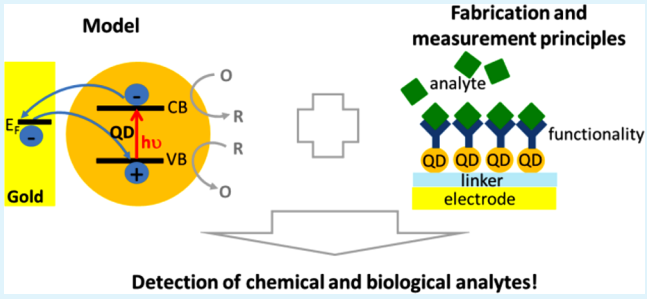

KEYWORDS: *photoelectrochemistry, quantum dots, nanoparticles, photocurrent, sensors*

1. INTRODUCTION

Quantum dot (QD)-based sensors for chemical and biological detection are presently a technological hot topic[1−8] because of the special optical and electronic properties of the component QDs[9−15] plus the possibility to relatively easily functionalize them with a wide variety of biological as well as for other important applications relevant molecules.[10,16−18] In principle, there are several ways that one may take advantage of the optical and electronic properties of QDs to design analytical methods for the detection of chemicals and biomolecules. This review focuses on sensors based on an electronic output, which consist of QDs immobilized on a conductive electrode. These systems can generate photocurrents which are sensitive to the chemical environment of the surrounding solution (see Figure 1). Although optical transducers based on fluorescence, fluorescence resonance energy transfer (FRET), chemiluminescence resonance energy transfer (CRET), and other mechanisms are already widespread,[1−4,19−38] the area of QD-based photoelectrochemical sensors has recently evolved into a rather new and important branch of biosensing, as many of their properties are advantageous when compared to the other sensor types. For example, even though they are still model systems, they are easy to operate, because they yield an

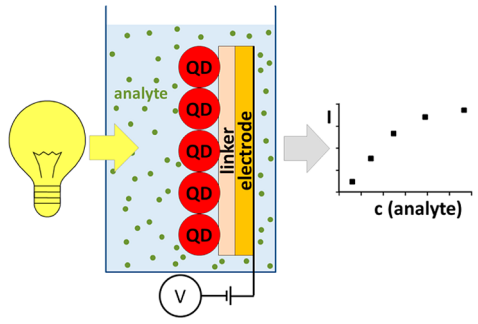

Figure 1. Schematic representation of a QD-based photoelectrochemical sensor. QDs are immobilized by a linker to an electrode, which is placed in a solution. Upon illumination of this electrode, a photocurrent is generated depending on the type and concentration of the analyte in the surrounding solution.

Special Issue: Forum on Biomedical Applications of Colloidal Photoluminescent Quantum Dots

Received: November 27, 2012
Accepted: March 14, 2013
Published: April 3, 2013

electronic output without the necessity to purchase expensive optical equipment. In addition to the potential applied, the impinging light can provide a means for controlling the desired reaction.

Furthermore, QD-based photoelectrochemical sensors have the following advantages: (1) As QDs serve as "pumps" for the charge carrier transfer between the conductive electrode and the redox agent (oxidant and reductant) through tunneling processes, one can achieve photoelectrochemical sensors with a fast response and high sensitivity. Through further coupling with biocatalytic reactions, this leads to the possibility to detect certain substances that cannot be detected using common optical property based analytical methods. (2) Only small dark-currents are observed in QD-based systems, because the immobilization layer, which links the nanoparticles to the electrode in most cases, blocks the access of substances to the electrode surface and thus, attenuates alternate electron transfer reactions. Under illumination this situation changes significantly and redox reactions can occur, thus the QDs play a key role as photoactivators of the sensor. Due to the broad absorption spectra of the QDs their photoelectrochemical sensor systems can be excited by a common white light source. This enables the design of simple, cheap, and portable sensor systems. (3) QD-based photoelectrochemical sensors can easily be extended to light-addressable sensors by the spatially resolved illumination of a selected area of the electrode provided that a spatially resolved immobilization of the recognition elements can be performed. As an extension of this strategy it should be possible to obtain spatially resolved coding or multichannel detection.[39] Compared to the traditional Si-based light addressable sensors,[40] QD-based light addressable sensors can potentially possess a higher lateral resolution, because the photoexcited electron−hole pairs should diffuse less within the semiconductor layer.[41−43] (4) The use of QDs opens the possibility to efficiently chemically couple additional moieties to the QDs, e.g., biomolecules.

As may be gleamed from the above, the great potential of QD-based photoelectrochemical sensors is clear. Because many recent reviews have already focused on QD-based optical sensors,[3,15] in this review, we focus our attention on the photoelectrochemical applications of QDs for chemical and biological detection. Once the functional principle and some advantages of these systems have been laid out, we describe several fabrication routes developed within recent years. In the sections that follow, the state-of-the art in the detection of chemicals and biomolecules is described and the broad range of molecules already detectable by QD-based photoelectrochemical sensors is presented. Finally, an overview to conclude the actual observations is given and future perspectives are discussed.

1.1. Functional Principle. As a general rule, this type of photoelectrochemical sensor consists of QDs immobilized onto an electrode, which in most cases is achieved via an organic linker layer. Subsequent to the excitation of the QDs and under the application of an appropriate potential, electrons can tunnel from the electrode to the valence band of the QDs, and electrons present in the conduction band of the QDs can tunnel to oxidant molecules (electron acceptors) in the surrounding solution. Hence, in such a case, the cathodic photocurrent generated monotonically increases with increasing concentration of the oxidant present in solution. By contrast, if reducing molecules (electron donors) exist in solution, tunneling of electrons from the solution phase to the valence band of the QDs and of electrons from the conduction band to the electrode occurs. It can therefore be seen that both the direction and the amplitude of the resulting photocurrent are determined by the concentration of molecules (to be detected) and by the bias potential applied to the electrode. A commonly employed schematic depicting the detection principle is shown in Figure 2. As previously mentioned,

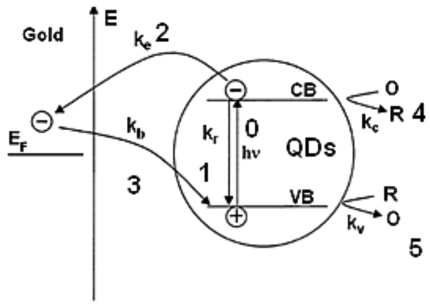

Figure 2. Energy diagram of photoinduced charge carrier transfer in a QD-based photoelectrochemical system corresponding to the models presented within refs 44−47. k_r is the rate of the relaxation pathway, k_e and k_b are the electron transfer rates from the conduction band to the electrode and from the electrode to the valence band, respectively. k_c and k_v are the transfer rate from the conduction band to a molecule in solution (O) being reduced to R, and the transfer rate from a molecule (R) in solution being oxidized (to O) to the valence band, respectively.

upon illumination, electrons in the QDs are excited, which subsequently have the possibility to either tunnel to the gold electrode (with a transfer rate k_e (2), or to solution and reduce oxidants (transfer rate k_c (4). Generated excited state holes can be filled by electrons tunneling from the electrode to the QDs (rate k_b (3) or tunneling from reductants in solution to the QDs (rate k_v (5). Hence, several electron transfer processes (2−5) are competing with the excitation process (0) and the recombination process (1), altogether yielding a net photocurrent. The amplitude, shape, and direction of this photocurrent will be controlled by the kinetics of each individual step.

The rates k_e and k_b, which are tunneling rates between the QDs and the electrode, strongly depend on the energy barrier height (determined by the linker material), on the barrier distance (determined by the thickness of the linker material), as well as on the difference between the Fermi level of the gold electrode and the energetic bands of the QDs.[48] Hence, k_e and k_b are influenced by the chemical composition and thickness of the linker, the applied potential, the size or material composition of the QDs and the surface modification protocol used for creating the interface with the solution. k_v is the electron tunneling rate from the reductants in solution to the photoinduced holes in the valence band of the QDs. k_c is the transfer rate of photoinduced electrons from the conduction band of the QDs tunneling to the electron acceptors O in solution. Consequently, k_v and k_c are influenced by the concentration of donors and acceptors in solution and by the surface properties of the modified QDs.

From a comparison between the theoretical models,[46,49] simulations,[46,47] and experimental results,[41] it can clearly be seen that the energetic position of the conduction band and the valence band of the QDs (determined by the size and composition of the QDs), the distance between the gold electrode surface and the QDs (i.e., the thickness and conductive properties of the immobilization layer), the position

of the Femi level in the gold electrode (i.e., the bias potential), and the concentration of the redox agent in solution will all influence the output characteristics of the photocurrent. Therefore, one has to take particular account of all these parameters when designing an appropriate QD-based photoelectrochemical sensor. When all other parameters remain constant, the amplitude of the photocurrent will follow the charge transfer rates as determined by the redox agent concentration (k_v or k_c) at the respective bias potential. Hence, it is reasonable that QD-based photoelectrochemical detection of different molecules is quantifiable by measuring the amplitude of the photocurrent.

All theoretical studies describe the same basic concept, with the exception of the description of the role surface states in the QDs, which are commonly referred to as "traps".[44−47,50−53] Traps are energetic states that usually appear because of the break in symmetry at the surface of QDs and which result in artifacts such as vacancies, defects etc., which can be located within the band gap of the QDs.[54−56] Once such states exist, excited electrons (or holes) may occupy them (meaning they are "trapped") and, if many such states are present and/or trapping events occur with a high probability, significant depopulation of the conduction band (or the holes in the valence band) can result. For applications in which QDs are used as fluorescent dyes, usually efforts are undertaken to minimize the amount of surface traps that occur because such states result in a reduction of the photoluminescence quantum yield. However, in the field of QD-based photoelectrochemical sensors, the role of trap states is hotly debated and often controversial. In recent publications, two different kinds of models regarding the role of trap states can be found with the frequently discussed controversial question being whether the direction of the photocurrent follows the applied bias potential or not. Using time-resolved photoelectrochemical measurements, several research groups independently obtained similar charge transfer models for QD-based photoelectrochemical setups with gold and ITO electrodes.[44,45,50−53,57−62] According to their observations, for QDs of different materials and different charge carrier trapping properties, different models are required to be developed. For CdS QDs, it has been demonstrated that hole traps play the main role in the photocurrent generation. Here, the direction of the photocurrent did not follow the bias potential, even though the amplitude and shape profiles did. In a separate study obtained for PbS QDs, for the same bias voltage range, different directions in the photocurrent were observed. In a further work, published by Nakanishi et al., multilayers of QDs on gold electrodes were characterized by Fourier transform infrared reflection absorption spectroscopy (FT-IRRAS)[63,64] where a similar behavior was observed, namely that only positive photocurrents resulted for both positive and negative bias potentials at the electrode. The corresponding model, in which charge carrier trapping plays an important role for the resulting photocurrent, takes into account the more complex situation where traps are present. This model is an extension of that presented in Figure 2, which results from the combined studies within several other research groups.[2,41,65−72] In their observations, the direction of the photocurrent was clearly reversible and determined by the bias potential applied. Here, a bias potential more negative than the Fermi level resulted in a negative photocurrent, and a bias potential more positive than the Fermi level in a positive photocurrent. Also, for photoelectrodes with CdSe or CdSe/ZnS core/shell QDs, it was observed that the amplitude of the photocurrent followed the absorption spectra of the QDs, and that the direction of the photocurrent followed the direction of the bias potential.[69,73] This is highly indicative that in these cases, the photocurrents arose from electron hole pairs undisturbed by trap states.

One possible explanation for the many and varied observational discrepancies that one finds in the literature may be due to the use of QD materials of different quality especially with respect to the amount of trap states present. Interestingly, many of the older publications report on the importance of trap states, while more recent publications report more on the minor role of trap states, and is a change that may be considered to coincide with the development of improved QD synthesis routes which produce materials with higher photoluminescence quantum yields resulting from the presence of fewer defect states. The quality of the QDs and the type of surfactant molecules present at the QD surface crucially influence the occurrence (in terms of number and energetic level) of traps. The presence of a surface state can reduce the transfer rate to the electrode or to the redox molecule (depending on the type of trap state) and hence make the photocurrent become unidirectional, whereas the amplitude of the photocurrent will be influenced by the light intensity.

Despite the reported differences in the experimental results concerning the role of the trap states as described above, the possibility of photoelectrochemical detection of substances in solution is not prevented: it does not matter whether positive or negative potentials are applied or if the direction of the photocurrent is reversible or not under different bias voltages, the main observation remains, namely that the amplitude of the photocurrent depends on the concentration of the donor/acceptor compounds. However, there are some inherent disadvantages when surface states play the main role in a photoelectrochemical detection system. The first is that in the case where one type of QD is used, the system can only be used to either oxidize molecules or to reduce them. For example, Katz et al.[65] reported the simultaneous photoelectrochemical detection of both the oxidized and reduced states of cytochrome c employing only one type of QD by a simple variation of the bias potential. If surface states had played the main role in the charge carrier separation step, the photocurrent would not have been reversible. In that case, only the oxidized or the reduced cytochrome c species would have been detectable. Second, if the photocurrent is dominated by trap states that are not size-dependent, multichannel detection or coding parallel analysis based on the size-dependent properties of the QDs in a photoelectrochemical sensor system cannot be achieved. Therefore, for such kinds of applications, it is strongly recommended to avoid the occurrence of surface states when designing and fabricating QD-based photoelectrochemical sensors. However, these trap related issues are solvable through the use of well passivated state of the art QDs (e.g., core shell or core multi-shell QDs) and are expected to further diminish in their importance, especially when one views the rapid progress made within the colloid chemical synthesis of QDs over the past decades.

1.2. Advantages. As described in the previous section, QDs act as a mediator in the electron transfer between molecules and a conductive electrode, with the photocurrent scaling as a function of the analyte concentration. As a consequence, some biomolecules such as nicotinamide adenine dinucleotide (NADH) or even proteins become detectable.[1,66] Besides the above-described advantages of using light as a

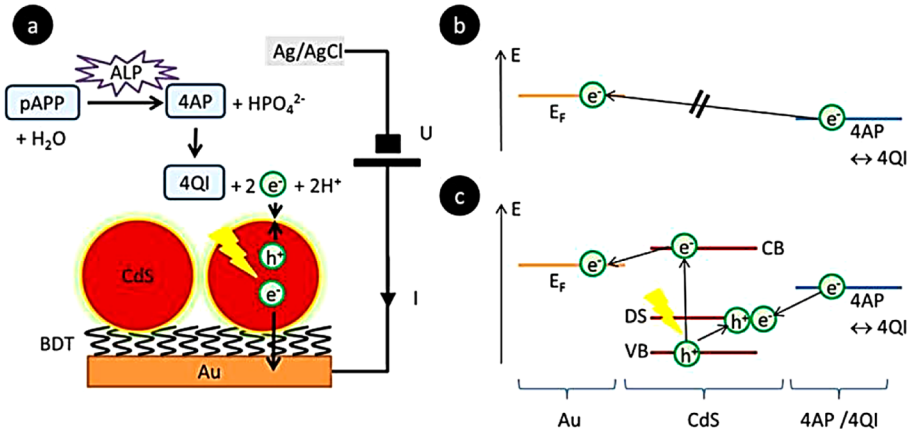

Figure 3. (a) Detection scheme for indirect detection of *p*-aminophenyl phosphate by QDs immobilized on a gold electrode. The energy schemes show that (b) in the absence of light, no current is detected, whereas (c) under illumination, charge transfer can happen, which leads to the generation of a photocurrent. Reprinted with permission from ref 76. Copyright 2011 BioMed Central.

sensorial read-out tool, in some cases QD-based photoelectrochemical sensor systems can provide higher sensitivities and lower detection limits than metal nanoparticle or QD-based optical sensors or even conventional electrochemical sensors.[74,75]

a. Low Limit of Detection. Most of the reported sensing schemes based on QDs work in a similar concentration range to that of alternative systems that use optical or electrochemical transduction principles. However, some studies have devoted much effort to showing the potential of using photoelectrochemical detection with respect to their very low detection limits.

In a report published by Yildiz et al.,[74] electrochemical and photoelectrochemical detection of tyrosinase (an indicative marker for melanoma cancer cells) activity were realized by using Pt nanoparticles and CdS QDs as electrocatalytic labels and photoelectrochemical reporter units, respectively. The limit of detection (LOD) of tyrosinase was tested and compared with other analytical techniques such as QD-based optical sensors, ion-sensitive field-effect transistor (FET) devices and quartz crystal microbalance (QCM). While the Pt nanoparticle based electrochemical method was shown to be the least sensitive method among the three electronic sensors for analyzing tyrosinase, the photoelectrochemical detection of tyrosinase activity was demonstrated to possess the highest sensitivity and showed the lowest detection limit. Golub et al.[75] have exploited a common aptasensor configuration for the electrochemical and photoelectrochemical detection of cocaine. Here the gold electrode was functionalized with one aptamer subunit, while another aptamer subunit was linked either to a Pt nanoparticle, a Au nanoparticle or a CdS quantum dot. In the presence of cocaine, the close proximity of the electrode to the respective nanoparticle was detectable either via the reduction of H_2O_2 (in case of Pt nanoparticles), via the changes in photocurrent in the presence of triethanol amine (in case of CdS QDs) or via the changes in the reflectance spectra caused by the changes in the surface plasmon resonances (in case of Au nanoparticles). For the CdS-based detection of cocaine, the photocurrent was generated by the ejection of the conduction band electrons into the electrode, and the filling of the valence-band holes by a charge transfer from a sacrificial electron donor in the vicinity. The intensities of the photocurrents were controlled by the amount of supramolecular cocaine-aptamer complexes attached to the electrode. All three configurations revealed a common advantage over the available aptasensors due to a reduced background signal. Also in this investigation the photoelectrochemical method provided the lowest LOD of cocaine corresponding to 1×10^{-6} M compared to 1×10^{-5} M (electrochemical detection with Pt nanoparticles). The two articles described above display the first proof that for certain arrangements and good-quality quantum dots, the limit of detection can be significantly lower for QD-based photoelectrochemical sensors than for different optical or electrochemical QD-based sensor systems.

b. Low Working Potential. Khalid et al.[76] designed a photoelectrochemical sensor for the indirect detection of *p*-aminophenyl phosphate (*p*APP) that can operate at rather low potential (see Figure 3). The sensor was based on the electrochemical conversion of 4-aminophenol at a QD modified electrode under illumination. First, in an enzymatic reaction, *p*APP was degraded to 4-aminophenol. Upon illumination of the QDs, electron hole pairs were generated, so that the photoexcited holes from the valence band of the QDs lead to oxidation of the 4-aminophenol, while the photoexcited electrons were transferred to the Au electrode. An oxidation photocurrent which was dependent on the presence of 4-aminophenol could thus be detected. In the absence of QDs, oxidation of 4-aminophenol by the gold electrode did not take place if the applied bias potential was not sufficiently high. However, with a QD interlayer, detection could already be achieved at low working potentials. This observation supports the general assumption that with the correct arrangement within the QD-based photoelectrochemical sensors, the working potential and hence the energy consumption can be reduced significantly in certain cases. Another example in this direction is the oxidation of NADH at potentials around 0 V vs Ag/AgCl.[35]

2. FABRICATION METHODS

As previously mentioned a QD-based photoelectrochemical sensor usually consists of an electrode (gold, TiO_2, indium tin oxide (ITO), fluorine doped tin oxide (FTO), carbon, etc.) onto which the QDs are immobilized. Optically transparent electrodes have the advantage that the illumination can be applied from the back side which reduces any unwanted photochemical or photophysical interactions with the solution.

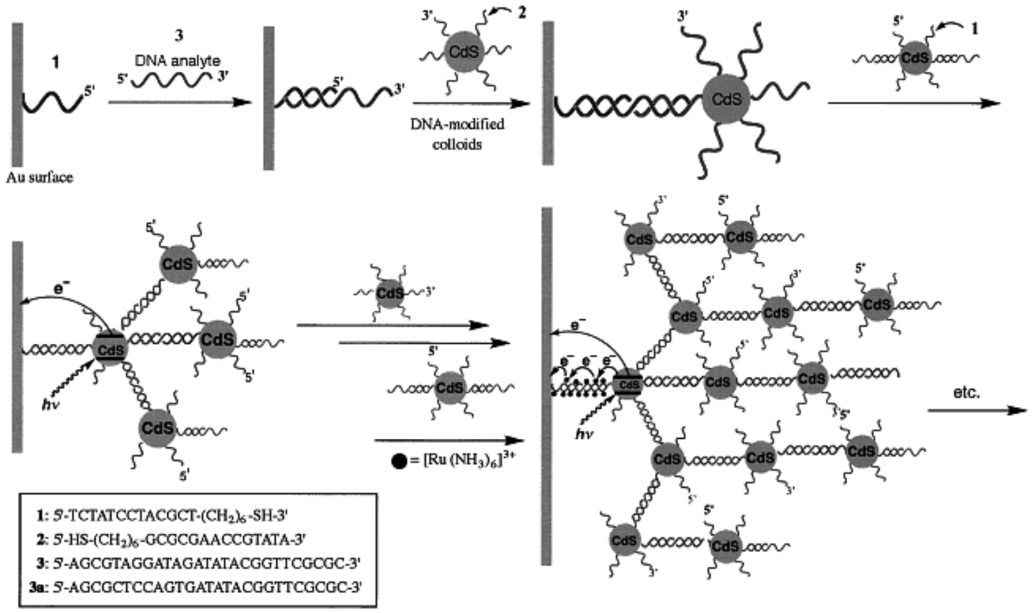

Figure 4. Organization of oligonucleotide/DNA-cross-linked arrays of CdS nanoparticles and photoelectrochemical response of the nanoarchitectures. Reprinted with permission from ref 73. Copyright 2001 Wiley−VCH Verlag GmbH.

However, usually these types of electrodes are relatively rough, which can be disadvantageous for certain applications.

QD-based photoelectrochemical sensors are normally fabricated in three steps: synthesis and modification of the QDs, immobilization of a linker molecule layer and deposition of the QDs onto the electrode. The present review does not address the synthesis of QDs and their surface modification. Instead, it is specifically about the immobilization of the QDs on the electrodes, which is a very important parameter in the fabrication of high-end photoelectrochemical sensors, and which will be discussed in more detail in the following subsection.

2.1. Assembly Methods of QDs onto Electrodes. To immobilize the QDs on a conductive electrode, chemical assembly methods onto a variety of different insulating or conducting materials can generally be employed. For the connection of QDs to gold electrodes, linker molecules with two thiol groups such as alkanedithiols,[63,64] 1,4-dithiane,[45,66] 1,4-benzene-dithiol,[41,69] 1,6-hexanedithiol,[45] stilbenedithiol,[72] etc., have been demonstrated to be advantageous because thiol groups bind strongly to both the QDs and the gold surface. For linking QDs to TiO_2 or indium tin oxide (ITO) electrodes, silane molecules with an additional functional group such as (3-aminopropyl)trimethoxysilane or (3-mercaptopropyl)trimethoxysilane are commonly used.[53,77]

Several research groups have already attempted to provide a common model to explain the QD/self-assembled monolayer (SAM)/electrode structure in a number of different ways and with different analytical tools.[41,44−47,49−53,57−62,64,68,78−87] The general photoelectrochemical knowledge gained through understanding this kind of system has broader implications since similar structures can be found in use for applications such as solar cells with high photon conversion efficiencies. Hence, many solar energy research-based groups have also intensively studied such QD/SAM/electrode systems, which has led to an improvement in our understanding of QD-based photoelectrochemical sensors.[88−90]

Because of its capacity as an in-series component the type of linker molecule used is of utmost importance. This can be seen for example from the works of Bakkers et al.[50] and Yue et al.,[41] which describe how, in absence of thiol molecules the QDs are not tightly bound to the electrodes, and that the length of the SAM molecules significantly affects the charge transfer rate. The presence of too great a distance within these mostly insulating materials strongly reduces or even prevents the photocurrent, since the distance-dependent tunneling processes are attenuated. Furthermore it should be mentioned that good passivation resulting from a high-quality SAM is frequently not achieved. For example, short chained dithiol molecules have been observed to not form SAMs, and the binding of both thiol functional groups to the gold electrode also needs to be prevented.[72] For these reasons, it is clear that the composition and thickness of the linking material as well as the quality of the SAM formed is highly important for the quality of any resulting sensor system.[91]

Furthermore, densely packed layers of QDs on the electrode will provide a better performance than if the QDs are individually distributed. Therefore, a variety of nanoparticle assembly techniques has been developed such as the previously described assembly mediated by functional molecules, embedding the QDs in polyelectrolyte multilayers (so-called layer-by-layer systems), or directed assembly[92] e.g. by means of block-copolymers.[93−95] To achieve optimum tuning of the layer properties, the nanoparticle assemblies have been studied intensely by different measurement techniques such as cyclic voltammetry,[41] scanning tunneling microscopy,[79] X-ray photon spectroscopy,[63] atomic force microscopy,[96] quartz crystal microbalance,[97] and surface plasmon resonance.[75]

Apart from monolayers of QDs on electrodes, the performance of multilayered systems has been frequently studied in QD-based photoelectrochemical sensing systems. Generally it has been found that multilayered deposition of QDs produce larger and more stable photocurrent amplitudes which scale with the number of layers.[63,64,73,75,98] Chemical linkers were employed so that layers of metal NPs or carbon nanotubes

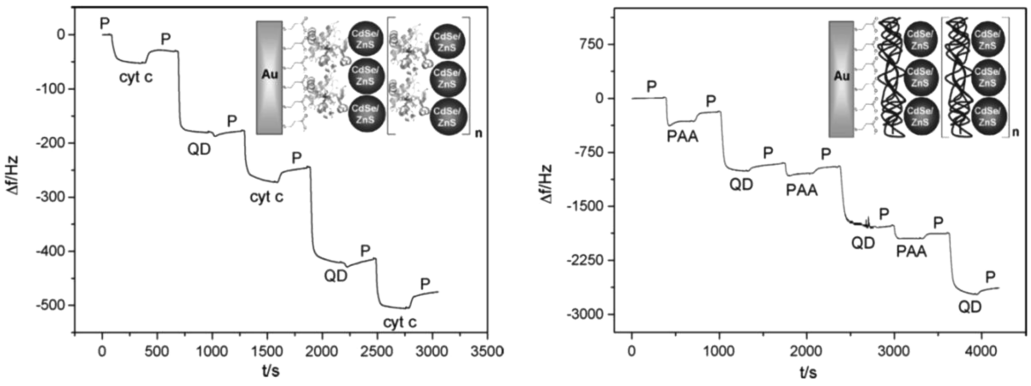

Figure 5. Multilayer formation with (left) cytochrome c and (right) PAA both exhibiting a positive surface charge and mercaptopropionic acid-modified CdSe/ZnS QDs exhibiting a negative surface charge. The assembly processes were followed by quartz crystal microbalance measurements in a flow cell. The insets display the respective setup scheme. Adapted with permission from ref 102. Copyright 2012 Elsevier.

could be included between the QDs and the electrodes, which was observed to enhance the charge carrier transfer and hence improve the photocurrent.[99,100] Golub et al.[13] and Willner et al.[73,75] successfully employed duplex DNA chains as linking material to construct mono- and multilayers of QDs. Because the conductivity of the stacked systems in dsDNA is limited, intercalators were added to the DNA, which lead to a significantly improved conductivity. Alternatively, redox active shuttle molecules or substances that interact electrostatically with DNA can also be used. The immobilization and enhancement process is shown in the diagram in Figure 4.

In addition to the assembly methods based on covalent linking, electrochemical deposition techniques,[22,101] physical methods (such as spin coating),[41] and electrostatic adsorption (such as layer-by-layer assembly of positively charged polyelectrolytes and negatively charged QDs[41,47]) have been widely studied. Polyelectrolyte assisted layer-by-layer methods were found to be an interesting approach for a number of reasons. First, the polyelectrolyte plays the role of a linker and at the same time provides advantageous conditions for interparticle electron transfer. Second, a polyelectrolyte assisted layer-by-layer method opens the possibility to further integrate additional species. For example, metal ions can be included which have been shown to result in a higher photocurrent stability.[47] Other approaches are to embed charged proteins, which can be tailored to yield defined reactions with certain analyte molecules[102] or even to include different types of functional nanoparticles.

Göbel et al.[102] have made a comparative study between the photocurrents of two different QD multilayer systems, whereby one system was constructed by electrostatic adsorption of the redox protein cytochrome c and the other by a positively charged polyelectrolyte (poly(allylamine hydrochloride), PAA) (see Figure 5). Although both photocurrents were observed to follow the number of deposited QD layers, the Au/(cytochrome c/QDs)$_n$ system showed only a slight enhancement of the photocurrents since the cytochrome c cannot facilitate the electron transfer between the QD layers. However, the Au/(PAA/QDs)$_n$ system provided a proportional increase in the photocurrent with the number of deposited layers, which was explained by the fact that PAA ensures short distances between the QDs and thus allows a rather undisturbed interparticle electron transfer. This example also shows that the choice of materials employed for the construction of the QD multilayers by electrostatic adsorption plays a very important role in yielding a high photocurrent output.

2.2. Improving the Charge Carrier Separation. In order for the sensors to obtain higher photocurrents and sensitivities, improving the separation efficiency of the photogenerated electron and hole pairs from the QDs is crucial. In the following paragraph, approaches to achieve this are discussed.

As explained in section 1.1, charge carrier transfer competes with the recombination process and since the recombination process is very fast, it is likely that photoinduced electrons and holes cannot be efficiently separated, which limits the photocurrent. As mentioned above, electron or hole donors such as ascorbic acid can be introduced to the system in order to improve the electron hole separation. In ref 71, methylene blue is described as being able to improve the charge carrier separation. Methylene blue is also an effective organic electron transfer mediator used for sensors and biosensors. The application of methylene blue not only enabled the measurement of higher photocurrent values, but photocurrents at lower QD concentrations were also observed. Of course, such reactions interfere with a direct analyte conversion at the QDs, but they are valuable for the detection of QD labels bound to the surface by a biospecific recognition event.

To improve the separation efficiency and therefore the photocurrent, composite QD assemblies and hybrid nanostructures have recently been used and studied. Metals such as gold nanoparticles and semiconductor nanomaterials (nanoparticles, nanowires, carbon nanotubes, TiO_2, SnO_2, etc.) have all been used to increase the separation efficiency of photoinduced electron hole pairs. Two different kinds of hybrid nanosystems in particular have been tested: the first type are nanoheterostructures arising from special types of synthesis,[72] e.g., dimeric nanoobjects of which at least one domain consists of a semiconducting material. The second type of hybrid nanosystem arises from assembly methods of separate semiconductor QDs together with nanoparticles from different materials e.g. metals.[100,103,104] The combination of two different nanomaterials in a nanoheterostructure by synthetic methods (such as the synthesis of CdS-SnO_2 nanoheterodimers) can result in an increase in the probability of charge carrier separation in the system, and hence in improved photoelectrochemical properties. Here, the conduction band electrons in the CdS-particles were transferred to the conduction band of the SnO_2, resulting in a delocalization of the electron and the hole (see diagram in Figure 6). Examples

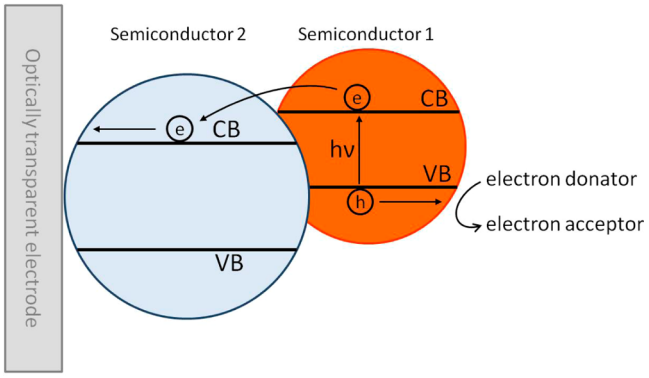

Figure 6. Schematic drawing of the suppression of charge carrier recombination in a semiconductor nanoheterostructure with properly aligned band gaps. In the excited state, electrons are transferred from the conduction band of semiconductor 1 to the conduction band of semiconductor 2. Because of the spatial separation of the electrons and holes, direct recombination is suppressed. The electron is then transferred to the electrode, and the hole (which remains in semiconductor 1) is filled by an electron donor from the solution.[108]

of nanoheterostructures for the charge-carrier separation are nanoobjects composed from CdS and Au,[81] CdS and carbon nanotubes[105] or graphene,[106] CdSe and C60 molecules,[107] as well as the afore-mentioned system from CdS and SnO_2.[108]

Similarly, metal nanoparticles, semiconductor nanomaterials and organic molecules can be deposited on top of QDs or between the QDs and the electrodes in order to generate photocatalytic activity, which is attributed to the effective separation of the excited electrons and holes which have been formed in the semiconductor domain of the hybrid system. Examples of such systems are: CdS QDs on TiO_2 nanocrystallites[109] or CdS on TiO_2 electrodes,[110] CdS QDs and Au NPs on electrodes,[100,111] CdS/ZnO hierarchical nanospheres,[112] and QDs in combination with bipyridinium or cyclodextrin.[91,113,114] Also, CdS/carbon nanotube composites have been used in order to increase the charge carrier separation rate (see Figure 7).[99,105,115] In the approach of

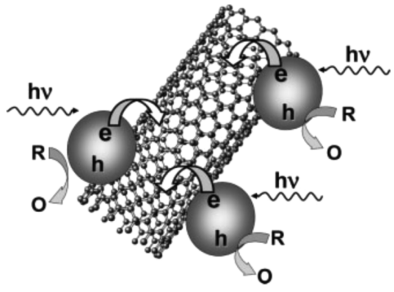

Figure 7. Charge-transfer interaction between photoexcited CdS nanoparticles and single-wall carbon nanotubes. Reprinted with permission from ref 105. Copyright 2005 Wiley−VCH Verlag GmbH.

Robel et al. where CdS−carbon nanotube nanocomposite suspensions were used, an effective electron transfer from the excited CdS QDs to the single-walled carbon nanotubes[105] was confirmed by transient absorption spectroscopy, which indicated an efficient electron separation efficiency. A different approach involves chemically assisted assembly methods to include carbon nanotubes between the QDs and the electrode.[99,115] This can be obtained for example by exploiting thiol or amino groups. The efficiency of such a system can be seen from the work of Sheeney-Haj-Ichia et al.[99] in which high photocurrents are reported. Here, furthermore, it was suggested that the length of the carbon nanotubes played a major role for the amplitude of the photocurrents, and it was presumed that the defects in the carbon nanotubes affected the extent of charge carrier separation. However, recent results have revealed that CdS/graphene hybrid nanostructure can exhibit even better charge separation properties than single-walled carbon nanotube/QDs systems.[116,117] In a previous article of Sheeney-Haj-Ichia et al.,[100] Au NPs were employed to enhance photoinduced charge separation. In either case, whether the Au NPs were inserted between the QDs and the electrode, or whether the Au NPs were immobilized on top of the QD layer, enhanced photocurrents (compared to a simple CdS-QD only interface) were observed, which was attributed to an increase in the charge carrier separation in the Au/CdS hybrid system. However, the efficiency differed with respect to the position occupied by the Au NPs within the assembly. In this study, the insertion of Au NPs between the electrode and the QDs led to better photoelectrochemical properties than other Au-CdS arrangements.

From the aforementioned studies, it can be seen that carbon nanotubes, Au NPs, TiO_2 NPs, etc., can be used both in nanoheterostructures, hybrid or combined systems to improve the charge carrier separation and hence increase the photocurrent. The difference between these two types of setup is that the nanoheterostructures provide better charge separation because of the tight connection of the two material domains within one particle, but on the other hand hybrid structures resulting from the assembly of different individual nanocomponents are much easier to achieve. It should be pointed out that although a variety of different nanomaterials can enhance the charge carrier separation efficiency; the location of these nanomaterials inside the QD-based photoelectrochemical system is crucial, especially in the case of hybrid nanoassemblies. A change in their position will lead to a change in the separation efficiency.

2.3. Reducing the Drift. Unstable photocurrent output (drift) is one shortcoming of QD-based photoelectrochemical sensors.[41,110,118] There are two main causes for the drift of the photocurrent output. The first is a poor connection between the QDs and the electrode, whereas the second is charging and discharging (also called photocorrosion) of the excited QDs. In the following paragraphs, these two causes of unstable photocurrents will be discussed in more detail.

a. Improving the Connection between the QDs and the Electrode. Unstable photocurrents can occur when QDs are disassembled from the electrode during the measurement, which results for instance when the link between the QDs and the gold electrode is not strong enough. This observation was confirmed during scanning tunneling microscopy measurements, as described by Ogawa et al.[78] To prevent the disassembly of the QDs during the photocurrent measurements, different electrodes, self-assembly materials, and SAM methods have been studied in order to improve the link between electrode and QDs. Khalid et al.[72] compared the photocurrent stabilities from three different types of electrodes (Au@glass, mica and SiO_2) and for different SAM materials annealed at different temperatures. In this case, Au@SiO_2 provided the lowest drift, and stilbene dithiol SAMs heated at 300 K provided much better SAM results (highest order and lowest drift, most probably due to the strongest linking of the

QDs to the surface) than, for example, nonannealed stilbene dithiol SAMs.

Electrochemical assembly of a *p*-aminothiophenol-capped CdS QD monolayer on *p*-aminothiophenol-functionalized gold surfaces was described by Granot et al.[97] Using this method, the QDs were covalently bound to form a densely packed monolayer on the surface. Here, the cross-linker molecules additionally provided an improved photoelectrochemical performance, since the electron transport of the conduction band electrons by the aromatic cross-linker facilitated charge carrier separation, which lead to the generation of a higher photocurrent.

In addition to covalent and electrostatic binding of the QDs to the electrodes, assembly methods employing hydrogen bonding such as through complementary barbiturate - triaminodiazine[119] or specific guanine-cytosine (G-C) and adenine-thymine (A-T) interactions[120] have also been successfully introduced. This type of binding exhibits a high stability in aqueous buffer solutions. For example, the G−C and A−T bridging units immobilized the QDs on the electrode, and furthermore provided an efficient interface for the electron transfer. The work on hydrogen bond mediated assembly methods with QD layers on gold based on nucleic base pairing has been further extended by the research group of Itamar Willner.[121−123] Tel-Vered et al.[121] have shown the CdS programmed assembly of CdS QDs by means of DNA. This enabled control over the exact composition and orientation of the resulting nanostructure and hence over the tunneling distances, which lead to control over the intensities and directions of the resulting photocurrents.

Because of the limited electronic coupling of the DNA-bound QDs to electrodes and a rather low coverage of the electrode surface with semiconductor nanoparticles (the absence of a densely packed interface), the photocurrent between the DNA-immobilized QDs and the electrode is only moderate. Freeman et al.[122] and Gill et al.[123] described the intercalation of doxorubicin or methylene blue into duplex DNA chains that enhanced the charge transport through the DNA bridges. Here, the resulting DNA linker structure acted as a conductive pathway for the charge transport, which lead to higher photocurrents and to the possibility of switching the photocurrent direction by means of the potential applied on the electrode (see Figure 8).

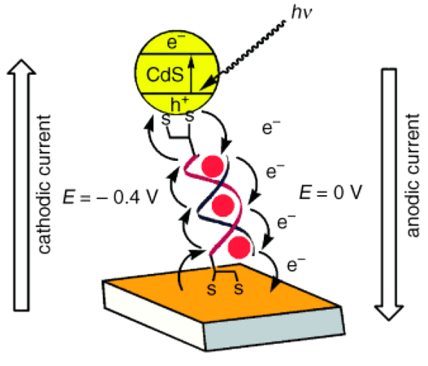

Figure 8. CdS nanoparticles immobilized on a gold electrode by a double-stranded DNA linker molecule. Depending on the redox state of an intercalating molecule, either anodic or cathodic photocurrents are detected. Reprinted with permission from ref 123. Copyright 2005 Wiley−VCH Verlag GmbH.

A different approach for significantly reducing the initial current drift and increasing the signal-to-noise ratio involved the addition of a polymer film on the top of the assembled QDs.[41] Again in this case the reduced drift was attributed to the fact that the polymer film prevents loss of the underlying QDs from the Au electrode. However, the changed chemical environment (due to the presence of the polymer) can also change the probability to populate surface states, or can reduce particle−particle communication. A similar observation was described by Pardo-Yissar et al.,[124] namely, that the presence of a capping on the QD layer leads to a more stable readout than the absence of such a capping.

b. Reducing the Charging and Discharging of the QDs. Another reason for the occurrence of drift is that the QDs can act as capacitors. According to the model described above, the photocurrent occurs because of charging (reduction by the electrode) and discharging (oxidation by the electrode) of QDs. When no electron donors or acceptors are in solution, the QDs will be continuously oxidized or reduced by the electrode, respectively. Because there are only a limited number of atoms in the QDs, and since the number of photoinduced electron−hole pairs is limited, the photocurrent changes over time.

To solve this problem, normally, we add different electron donors and hole donors to the solution such as triethanolamine,[73] Na_2S,[86] and Na_2SO_3[52] at pH 12, in order to warrant that the QDs stay in an electroneutral state and therefore reduce the output drift. Also, ascorbic acid can be added to overcome the charging and discharging problem of the QDs.[118] In that case, the ascorbic acid acts as an efficient and nontoxic electron donor for scavenging photogenerated holes under mild conditions and therefore inhibits the photocorrosion of the QDs. A different approach involves the use of redox pairs such as Fe^{2+} and Fe^{3+}, which are included in the QD layers (e.g., by the layer-by-layer method). These ions can play the role of electron donors and hole donors to avoid the QDs being totally oxidized or reduced.[47] It has to be mentioned here, that for analytical applications the presence of such substances is often not beneficial because they can interfere with the signal generation process. However, when the presence of QDs on the surface has to be analyzed, this effect can be advantageously applied.

Tanne et al.[125] have shown that the photocurrent is strongly influenced by the oxygen concentration. Oxygen plays the role of an electron acceptor. This is particularly visible under negative polarization and is influenced by the pH of the solution. The effect can be used for direct sensing, however, when other processes are studied, the removal of oxygen from the solution may be crucial for yielding a defined readout without interference by varying oxygen levels.

3. DETECTION OF CHEMICALS

QD-based photoelectrochemical systems have been widely used and studied in fabricating different kinds of sensors and new solar cells.[88] As the present review focuses mostly on the QD-based photoelectrochemical applications for chemical and biological detection, in this section, possible applications for such electrode systems are presented and discussed. QD-based photoelectrochemical sensors can be designed in basically two ways, namely either for direct or indirect measurement of the molecular concentrations.

There are two types of direct measurement setups. In the first, QDs are immobilized on the electrode and subsequently, appropriately modified. A potential is applied to the electrode,

so that electron transfer between the charge carriers of the excited state QDs and the corresponding and specific redox molecules can take place. The resulting photocurrent intensity corresponds to the concentration of substances to be detected.[66,76,126] Another direct measurement method is based on the principle that the analyte molecules can influence the binding properties of the QD layer on the electrode, which means that more or less QDs are immobilized on the electrode. This is related, for example, to the detection of binding reactions for which one partner is labeled with QDs. After the assembly, the photocurrent will follow the concentration of the molecules to be detected.[43,75] However, in certain cases, direct electron transfer between the QDs and molecules does not occur. Therefore, detection is realized by indirect measurements. For example, in many cases reaction byproducts can act as electron-acceptor or donor units which activate the photoelectrochemical operation of the QDs.[124] Another possibility resulting in an indirect measurement is the use of photoelectrochemical signal chains. In this way, a redox agent can act as a shuttle molecule between the QDs and the molecules or the catalyst, and thus enable the detection.[65,69]

In this section, sensors for a variety of such detectable molecules are presented employing either direct or indirect methods. One such molecular sensor is an ultrasensitive cysteine sensor constructed by Long et al.[70] In this setup, a Nafion film which was both chemically and photochemically inert was employed as the matrix to confine a stable spatial distribution of methyl viologen coated QDs by electrostatic interaction, which enabled the specific detection of cysteine. Methyl viologen was used to enhance the electron extraction from the excited QDs. The Nafion/CdS coated ITO electrode system was shown to be effective in the detection of cysteine with a fast response and high sensitivity: the cysteine lead to the highest response compared to all other amino acids investigated or to the blank solution, and the intensity of the signal was linear with respect to the cysteine concentration.

Another QD-based photoelectrochemical sensor, sensitive to metal ions such as Cu^{2+}, was reported by Wang et al.[127] where thioglycolic-acid-capped CdS QDs immobilized on an ITO electrode were used in order to develop a highly sensitive and selective photoelectrochemical sensor for Cu^{2+} ions. In the presence of Cu^{2+} ions in a triethanolamine solution, Cu_xS was presumably formed on the surface of the CdS QDs. This material transformation coincided with the generation of a lower energy level providing an effective pathway for the recombination of electron hole pairs in the QDs. Because of these electron−hole recombination centers (Cu^+ or Cu_xS), the electron transfer process from the QDs to the electrode was diminished, so that a decrease in the photocurrent was observed. Hence, the intensity decrease of the photocurrent was proportional to the Cu^{2+} concentration. On the basis of the same interaction principle, a new ITO/ZnO/CdS photoelectrochemical sensor for Cu^{2+} detection that displayed an even better performance was developed by Shen et al.[112] Hierarchical nanospheres consisting of a large ZnO domain and smaller CdS domains were attached to an ITO electrode for the selective sensing of Cu^{2+} ions. Here, the light scattering of the ZnO spheres and the heterointerface between the CdS domains and the ZnO provided an enhanced light absorption and charge separation, hence resulting in an improvement in the photocurrent intensity.

Further examples of photoelectrochemical sensors for small molecules are oxygen detection based on illuminated CdSe/ZnS quantum dots[125] or hydrogen peroxide detection. Because CdS and CdSe/ZnS QDs do not provide a suitable interface for hydrogen peroxide conversion, an alternative method was introduced by Khalid et al. who employed CdS-FePt nanoheterodimers to build H_2O_2 photoelectrochemical sensors working without the need for an enzyme.[72] CdS-FePt nanoheterodimers were linked to a gold electrode via a SAM of dithiol molecules yielding a FePt-CdS/SAM/Au structure. The CdS domain, which was in good electrical contact with the gold electrode, allowed for photocurrent generation. The FePt domain acted as a catalytic site for the reduction of H_2O_2. The H_2O_2 sensitivity of the FePt-CdS/SAM/Au electrode was observed to be higher than in the case when FePt NPs were coimmobilized with CdS QDs on gold (FePt/CdS/SAM/Au). This result furthermore opened a new way for applications of nanoheterodimers using photoelectrochemical detection.

4. BIOMOLECULAR DETECTION

4.1. Enzyme-Based Sensors. The first enzyme-based, indirect photoelectrochemical sensor described in this review is sensitive to acetylcholine via changes in the photocurrent which are dependent on the amount of acetylcholine present.[124] The sensor system described by Pardo-Yissar et al. is composed of acetylcholine esterase functionalized CdS QDs which are covalently linked to a gold electrode. The addition of acetylthiocholine to the system results in the acetylcholine esterase catalyzing the hydrolysis of acetylthiocholine to thiocholine and acetate. Thiocholine, as an electron donor, can be oxidized by the valence-band holes from the QDs, and the conduction-band electrons from the QDs can be transferred to the electrode, which results in the generation of a photocurrent, the amplitude of which is thus dependent on the amount of acetylthiocholine present in the system (or the presence of enzyme inhibitors).

Glucose can best be detected by photoelectrochemical QD sensors if combined with suitable enzymes in indirect measurements.[67,125,126,128] Schubert and co-workers[67] reported the direct sensitive detection of nicotinamide adenine dinucleotide (NADH) in the range of 20 μM to 2 mM at a rather low bias potential by using a photoelectrode system consisting of CdSe/ZnS QDs attached to gold. The indirect detection of glucose by signal chains became possible, since the glucose signal could be converted to NADH by electron transfer via the enzyme glucose dehydrogenase, and subsequently NADH was detected by an electron transfer to the illuminated QDs resulting in a photocurrent. Similarly, indirect detection of glucose was achieved by Tanne et al. by creating a signal chain from glucose via glucose oxidase and molecular oxygen via CdSe/ZnS QDs toward the electrode.[125] On the basis of the influence that the oxygen concentration has on the photocurrent, the enzymatic activity of glucose oxidase catalyzing the oxidation of glucose by the reduction of O_2 was evaluated. During illumination, the photocurrent was reduced as a result of the oxygen consumption. The sensing properties of this type of electrode were strongly influenced by the amount the enzyme on top of the QD layer, which was found to be easily adjustable using the layer-by-layer technique. Interestingly, a similar system—based on the oxygen sensitivity of the CdSe/ZnS electrode—could also be developed for the detection of sarcosin using sarcosin oxidase as biocatalyst.[129] The aforementioned glucose sensors are based on signal chains of glucose−glucose dehydrogenase-NADH-QDs or glucose−glucose oxidase-oxygen-QDs. However, the enzyme can also be

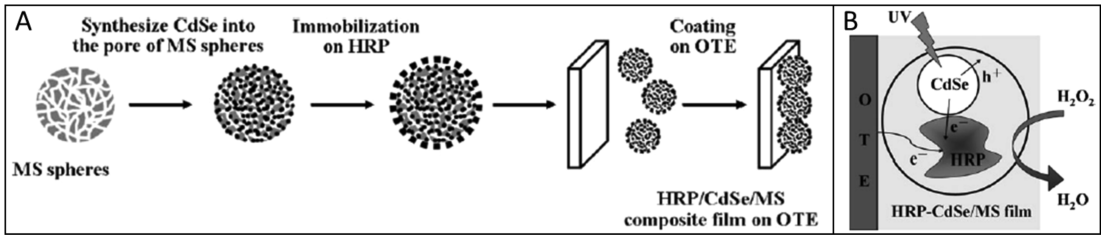

Figure 9. (A) Schematic diagram of the fabrication procedure of the horseradish peroxidase−QD−mesoporous silica/electrode composite film on an optically transparent electrode (OTE) and (B) charge transport scheme of the resulting system. Reproduced with permission from ref 133. Copyright 2010 Springer-Verlag.

coupled to an electrode by means of a shuttle molecule, which facilitates a mediated electron transfer from the biocatalyst. An example of this kind of detection principle can be found in a work by Zheng et al.[128] In this approach, a photoelectrochemical electrode was constructed by alternately depositing water-soluble CdSe-CdS QDs and a mixture of $[Co(phen)_3]^{2+/3+}$ and poly(ethyleneimine) on a TiO_2 electrode. An enhanced photocurrent and hence sensitivity was observed, which was attributed to the $[Co(phen)_3]^{2+}$ ions, capturing holes from the QDs and therefore suppressing electron−hole recombination. In this setup, the electrode was able to transfer charge carriers from the reduced enzyme, so that the obtained photocurrent depended on the concentration of glucose.

Zhao et al.[130,131] introduced 4-chloro-1-naphthol to an ITO/TiO_2/CdS/horseradish peroxidase photoelectrochemical biosensing system yielding high H_2O_2 sensitivity. The biocatalytic reaction yielded an insoluble product on the surface of the electrode, by which the photocurrent could be influenced. As a result, a so-called biocatalytic precipitation amplified photoelectrical detection of H_2O_2 was achieved. The resulting detection limit of 5.0×10^{-10} M from this indirect technique was much lower than that of previously reported direct photoelectrical sensors for H_2O_2 using TiO_2 nanotubes/horseradish peroxidase electrodes with a detection limit of 1.8×10^{-7} M,[132] but the sensor does not allow online measurements.

4.2. Sensors Based on Direct QD−Protein Interaction. QDs modified with a variety of different surface modifications and immobilized on a gold electrode have been employed to detect the small redox protein cytochrome c.[65,66,69] In a first example, CdSe/ZnS core/shell QDs were immobilized on a gold electrode by Stoll and co-workers[66] using dithiane as a linker molecule. Upon exchanging the original layer of hydrophobic surfactant molecules from the QD surface with a hydrophilic one (mercaptopropionic acid or mercaptosuccinic acid), oxidized cytochrome c could be detected under illumination at a negative bias potential. Katz et al. employed mercaptopyridine to modify the surface of CdS QDs, which were introduced in a QD-based photoelectrochemical sensor for the direct detection of cytochrome c.[65] Cathodic or anodic photocurrents were observed in the presence of oxidized or reduced cytochrome c, respectively. These results demonstrate control over the direction of the photocurrent generated by CdS QDs by means of the cytochrome c added in different oxidation states. Hence, it should be pointed out again, that the direction of the photocurrent is a very important element when designing biosensors, since it can provide useful information concerning the oxidation state of the biomolecules to be detected. Furthermore, other biomolecules could be detected by the indirect measurement of cytochrome c (as was shown by Katz et al.).[65] For example, by activating a secondary cytochrome c mediated biocatalytic process, lactate and NO_3^- were measured indirectly. In the presence of oxidized cytochrome c, the oxidation of lactate by lactate dehydrogenase was activated photoelectrocatalytically while generating an anodic photocurrent. Upon photoexcitation of the QDs, conduction band electrons were injected into the electrode, and at the same time cytochrome c was oxidized by holes from the valence band. The resulting oxidized cytochrome c mediated the lactate dehydrogenase oxidation. Similarly, the use of cytochrome c in its reduced form enabled the bioelectrocatalytic reduction of NO_3^- to NO_2^- by nitrate reductase, while generating a cathodic photocurrent. In a further set of experiments by Stoll et al., QDs with different surface modifications (mercaptopropionic acid, mercaptosuccinic acid and mercaptopyridine) were compared by measuring the photocurrent arising from the direct electron transfer of the redox protein cytochrome c.[69] For both oxidation states of cytochrome c, the use of 4-mercaptopyridine yielded the highest photocurrent and best electrode performance with respect to the facilitated protein electrode interaction. Therefore, 4-mercaptopyridine modified QDs were further investigated in a signal chain sensitive for superoxide radicals. The generation of superoxide radicals in solution was detected following the cytochrome c reoxidation at the illuminated electrode. Thus, the photocurrent correlated to the superoxide concentration in solution.

Another protein for which direct interaction with the QDs has been reported is horseradish peroxidase. Under illumination, the enzyme oxidized by H_2O_2 can be reduced back by excited state electrons from the conduction band of the QDs. Hence, the cathodic photocurrent is sensitive to the H_2O_2 concentration. Yang and co-workers[133] described the preparation of CdSe QDs inside mesoporous silica spheres, with subsequent preparation of a horseradish peroxidase-QD-mesoporous silica/electrode (see Figure 9). The CdSe/mesoporous silica composite was shown to exhibit an efficient charge carrier separation with recombination being minimized. A further example for horseradish peroxidase-based hydrogen peroxide sensing exploited TiO_2 nanotubes (see ref 132).

Other sensor systems were constructed for the detection of formaldehyde[134,135] and glutamate[126] with the respective dehydrogenase. For these systems, however, more mechanistic studies appear to be necessary in order to verify their potential dependence and analyze the possibility of direct analyte reactions.

4.3. Sensors for Binding Reactions. QD-based photoelectrochemical sensors can also be modified with antibodies for biochemical analysis of, for example, immunoglobulin. G.

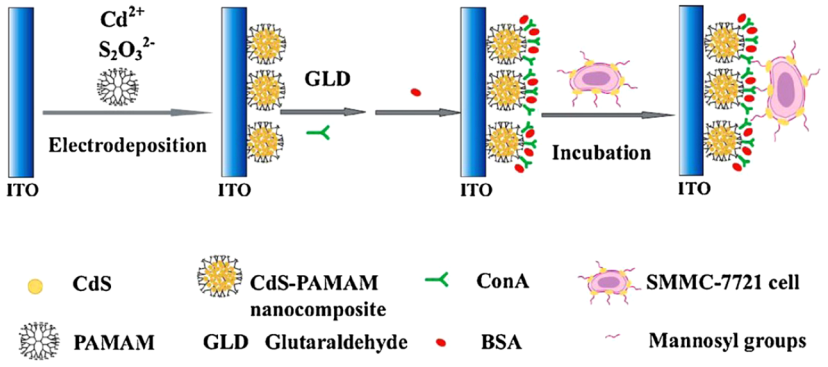

Figure 10. Detection of human hepatoma carcinoma cells by QD-based photoelectrochemical methods. Reproduced with permission from ref 22. Copyright 2010 Elsevier B.V.

Wang et al. have developed such a photoelectrochemical immunosensor[118] by preparing a multilayer film via layer-by-layer assembly of a polyelectrolyte and QDs onto an ITO electrode and by attaching goat antimouse immunoglobulin G to the QDs. The immunoglobulin G concentration was measured through the decrease in the photocurrent intensity, which is due to the increase in steric hindrances upon immunocomplex formation. A detection limit of 8.0 pg/mL at 0 V (vs. Ag/AgCl) was achieved. A similar method was used to detect α-fetoprotein antigen by Wang and co-workers.[110] The photoelectrochemical immunosensor was developed by alternately dipping the TiO_2 modified ITO electrode into a $[Cd(NH_3)_4]^{2+}$ and S^{2-} solution repeatedly and coating with chitosan and α-fetoprotein antibodies. Linear responses to α-fetoprotein in the range of 50 pg/mL to 50 ng/mL as well as a relatively low detection limit of 40 pg/mL were achieved. The photoelectrochemical results for the detection of α-fetoprotein showed acceptable accuracy in five human sera, such that this methodology was found to be potentially attractive for clinical immunoassays. Another interesting system to be described is a photoelectrochemical thrombin sensor which includes layers of graphene to enhance the charge separation and increase the photocurrent. Zhang et al. developed a sensing strategy for the highly sensitive and specific detection of thrombin based on the use of a specific aptamer and a layer-by-layer assembly of poly(acrylic acid) functionalized graphene combined with positively charged CdSe QD (ITO/graphene/CdSe QDs).[117] This system exhibited a detection limit of 4.5×10^{-13} M and significantly higher photocurrents than in the absence of graphene. This photoelectrochemical sensor exhibited stable photocurrents even in the presence of a 10-fold excess of foreign proteins, such as immunoglobulin G, bovine serum albumin and lysozyme. One of the most promising applications for biosensing is cancer diagnosis via the detection of tumor markers. For example, tyrosinase (an indicative marker for melanoma cancer cells) activity was successfully detected with a QD-based photoelectrochemical setup by Yildiz et al. (as already mentioned above).[74]

In the QD-based sensors described so far, the amount of QDs mounted onto the electrode is constant during the operation of the sensor and the detected (photo)current is varied via the reactions induced in the presence of an analyte which somehow affects the electron transfer from or toward the QD (e.g., via the generation of oxidizable/reducible species). However, the following sensor systems are different, since here the detectable molecules will influence the immobilization process of the QDs on the electrode and hence lead to a variation in the amount of QDs at the electrode interface which in turn will vary the amplitude of the detected photocurrent. For example, as described in refs 73 and 121−123, DNA was employed to immobilize QDs on electrodes. Mismatch of the DNA will influence the consistency of the QD film attached to the surface and, by measurement of the photocurrent change, the DNA mismatch can be detected. DNA does not only function as a bridging unit for QDs, but in addition the duplex DNA can act as a matrix for the incorporation of an intercalator molecule, such as methylene blue, facilitating the charge transport through the DNA bridges. The intercalation of molecular units was observed to be perturbed by single-base mismatches. Hence, this kind of photocurrent-generating system can be employed as a tool for base mismatch detection in DNA, opening interesting and important future applications in DNA detection.[73,123] A powerful DNA mismatch concept was adopted by Baş et al.[43] Here, target ssDNA competed with QD-ssDNA conjugates. By monitoring the decrease in the photocurrent generated from the QD-ssDNA conjugate, quantitative determination of the target ssDNA was enabled.

Besides the detection of certain biomolecules, first results on the specific detection of certain cell types with QD-based photoelectrochemical methods have already been obtained. For example, a photoelectrochemical sensor for specific cell detection (Ramos cells) was developed by Zhang et al.[136] employing a layer-by-layer assembly of a positively charged polyelectrolyte and negatively charged QDs on ITO. The resulting electrodes were tested as sensors for the Ramos cells through the recognition of DNA aptamers which were covalently attached to the electrode. Even though the linear performance of this setup was observed only within 1 order of magnitude in cell concentrations (from 160 to 1600 cells/mL) with a detection limit of 84 cells/mL, this result displays a proof of principle for this kind of specific cell detection via QD-based photoelectrochemical devices. A different cell type that could be specifically detected is SMMC-7721 human hepatoma carcinoma cells.[22] The photoelectrochemical cell-sensor was fabricated by Qian et al. via the electrodeposition of poly(amidoamine) and QDs onto ITO and subsequent attachment of a layer of concanavalin A (see Figure 10). The concanavalin A specifically recognized mannosyl groups from the cell surface with the photocurrent intensity decreasing upon the cells binding to the photosensitive film. The cell concentration was detectable from 5.0×10^3 to 1×10^7 cells mL^{-1}.

Looking at all these different mechanisms as outlined in this section, it becomes obvious that the field of techniques available

Table 1. Overview of the Sensor Systems Discussed in This Review for Quantum-Dot-Based Photoelectrochemical Detection of Chemicals and Biomolecules[a]

type of analyte	type of QDs	detection mechanism	authors
Cu^{2+}	thioglycolic-acid-capped CdS QDs	direct	Wang et al.[127]
	ZnO nanospheres with CdS QDs	direct	Shen et al.[112]
O_2	CdSe/ZnS core shell QDs	direct	Tanne et al.[125]
H_2O_2	CdS-FePt heterodimer	indirect	Khalid et al.[72]
	CdS QDs	indirect	Zhao et al.[130,131]
	CdSe QDs inside mesoporous silica spheres	indirect	Yang et al.[133]
superoxide radicals	4-mercaptopyridine-functionalized CdSe/ZnS	indirect	Stoll et al.[69]
nitrate	mercaptopyridine-functionalized CdS QDs	indirect	Katz et al.[65]
cysteine	methyl-viologen-coated CdS QDs	direct	Long et al.[70]
actylthiocholine (+esterase inhibitors)	acetylcholine-esterase-functionalized CdS QDs	indirect	Pardo-Yissar et al.[124]
glucose	CdSe/ZnS core shell QDs	indirect	Schubert et al.;[67] Tanne et al.,[125] Zheng et al.[128]
sarcosine	CdSe/ZnS core shell QDs	indirect	Riedel et al.[129]
p-aminophenyl phosphate	CdS QDs	indirect	Khalid et al.[76]
lactate	mercaptopyridine-functionalized CdS QDs	indirect	Katz et al.[65]
cocaine	aptamer-functionalized CdS QDs	direct	Golub et al.[75]
tyrosinase	CdS QDs modified with tyrosine methyl ester	indirect	Yildiz et al.[74]
cytochrome c	mercaptopropionic-acid-functionalized CdSe/ZnS core shell QDs	direct	Stoll et al.[66]
	mercaptopyridine-functionalized CdS QDs	direct	Katz et al.[65]
DNA mismatch	CdS QDs	direct	Willner et al.;[73] Tel-Vered et al.;[121] Freeman et al.;[122] Gill et al.;[123] Bas et al.[43]
α-fetoprotein antigen	CdS QDs	indirect	Wang et al.[110]
thrombin	graphene/CdSe QDs layer by layer structure	indirect	Zhang et al.[117]
immunoglobulin G	CdS QDs	indirect	Wang et al.[118]
Ramos cells	CdSe QDs	direct	Zhang et al.[136]
SMMC-7721 human hepatoma carcinoma cells	CdS/poly(amidoamine) nanocomposite	direct	Qian et al.[22]

[a]The order of appearance is sorted by the type of analyte starting from ions and small molecules, via biomolecules, to cells.

in the detection of biomolecules is quite broad. Apart from many different direct measurements already conducted, a variety of indirect measurements e.g. of reaction byproducts or by utilizing the assistance of intercalating molecules have already been employed as strategies to circumvent the sometimes difficult to apply direct measurement techniques. In total, this has already resulted in a variety of biomolecules which can presently be detected using quantum-dot-based photoelectrochemical sensors (see Table 1), which as a research field is continuously being extended.

5. CONCLUSIONS

Concepts, fabrication methods, improvements, and applications of QD-based photoelectrochemical sensors have been described with the main focus being on biochemical detection. It can be seen that because of the light-directed read-out and the broad range of functionalization possibilities, QD-based photoelectrochemical sensors have great potential and a promising future for applications such as biosensing. The variety of molecules presently detectable can be seen from Table 1, which summarizes the systems described in this article. However, since QD-based photoelectrochemical sensors are still in their infancy, some challenges still remain among which are: (1) the variety of sensing concepts and applications in the detection of different molecules will have to be further expanded by designing more specific QD/biomolecule hybrid systems or special nanoheterostructure building blocks. (2) QD-based photoelectrical sensors need to be further developed in order to achieve multichannel detection sensors with an aim to finding applications, e.g., in drug screening or medical analysis. (3) As with developments in the fabrication of QD-based solar cells, methodologies should be sought such that QD-based photoelectrochemical devices that have a similar structure may be fabricated in the same way. This will be beneficial for commercial production and practical use. (4) So far, most QD-based photoelectrochemical sensors are based on the most commonly studied QD systems, which are unfortunately predominantly based on Cd or Pb compounds, both of which are accompanied by toxicity issues. To avoid this, particularly in medical diagnosis, more work will have to be done, in order to expand the already large array of materials, to include less toxic QD materials, examples of which are fluorescent metal nanoparticles, carbon dots, InP, or Zn-based materials. (5) Electrode developments for analytical purposes have to show the applicability of this new type of sensor in real samples. This is related to signal height and stability but also to interference-free measurements. Much progress has already been achieved in the pursuit of these developments, and there is presently no reason to expect that future developments will not aid in the delivery of the advances required to compete with or even surpass the performances of the present generation of sensor devices.

AUTHOR INFORMATION

Corresponding Author

*E-mail: nadja.bigall@pci.uni-hannover.de. Phone: +49 511 762-16068.

Author Contributions

The manuscript was written through contributions of all authors. All authors have given approval to the final version of the manuscript.

Notes

The authors declare no competing financial interest.

■ ACKNOWLEDGMENTS

Z.Y. is grateful for financial support from the National Natural Science Foundation of China (61001056), Natural Science Foundation of Tianjin, China (10JCZDJC15300). Parts of this work were supported by DFG (GRK 1782).

■ REFERENCES

(1) Luo, X.; Morrin, A.; Killard, A. J.; Smyth, M. R. *Electroanalysis* **2006**, *18*, 319−326.
(2) Gill, R.; Zayats, M.; Willner, I. *Angew. Chem., Int. Ed.* **2008**, *47*, 7602−7625.
(3) Algar, W. R.; Tavares, A. J.; Krull, U. J. *Anal. Chim. Acta* **2010**, *673*, 1−25.
(4) Freeman, R.; Willner, B.; Willner, I. *J. Phys. Chem. Lett.* **2011**, *2*, 2667−2677.
(5) Lei, J.; Ju, H. *Chem. Soc. Rev.* **2012**, *41*, 2122−2134.
(6) Amelia, M.; Lincheneau, C.; Silvi, S.; Credi, A. *Chem. Soc. Rev.* **2012**, *41*, 5728−5743.
(7) Deng, S.; Ju, H. *Analyst* **2013**, *138*, 43−61.
(8) Lu, Z. S.; Li, C. M. *Curr. Med. Chem.* **2011**, *18*, 3516−3528.
(9) Smith, A. M.; Duan, H.; Mohs, A. M.; Nie, S. *Adv. Drug Delivery Rev.* **2008**, *60*, 1226−1240.
(10) Parak, W. J.; Pellegrino, T.; Plank, C. *Nanotechnology* **2005**, *16*, R9−R25.
(11) Dabbousi, B. O.; Rodriguez-Viejo, J.; Mikulec, F. V.; Heine, J. R.; Mattoussi, H.; Ober, R.; Jensen, K. F.; Bawendi, M. G. *J. Phys. Chem. B* **1997**, *101*, 9463−9475.
(12) Hines, M. A.; Guyot-Sionnest, P. *J. Phys. Chem.* **1996**, *100*, 468−471.
(13) Peng, X.; Schlamp, M. C.; Kadavanich, A. V.; Alivisatos, A. P. *J. Am. Chem. Soc.* **1997**, *119*, 7019−7029.
(14) Gao, X.; Yang, L.; Petros, J. A.; Marshall, F. F.; Simons, J. W.; Nie, S. *Curr. Opin. Biotechnol.* **2005**, *16*, 63−72.
(15) Medintz, I. L.; Uyeda, H. T.; Goldman, E. R.; Mattoussi, H. *Nat. Mater.* **2005**, *4*, 435−446.
(16) Parak, W. J.; Gerion, D.; Pellegrino, T.; Zanchet, D.; Micheel, C.; Williams, S. C.; Boudreau, R.; Le Gros, M. A.; Larabell, C. A.; Alivisatos, A. P. *Nanotechnology* **2003**, *14*, 15−27.
(17) Rodríguez-Hernández, J.; Chécot, F.; Gnanou, Y.; Lecommandoux, S. *Prog. Polym. Sci.* **2005**, *30*, 691−724.
(18) Grodzinski, P.; Silver, M.; Molnar, L. K. *Expert Rev. Mol. Diagn.* **2006**, *6*, 307−318.
(19) Lin, C.-A. J.; Liedl, T.; Sperling, R. A.; Fernández-Arguelles, M. T.; Costa-Fernández, J. M.; Pereiro, R.; Sanz-Medel, A.; Chang, W. H.; Parak, W. J. *J. Mater. Chem.* **2007**, *17*, 1343−1346.
(20) Ma, X.; Tan, H.; Kipp, T.; Mews, A. *Nano Lett.* **2010**, *10*, 4166−4174.
(21) Zhang, F.; Ali, Z.; Amin, F.; Riedinger, A.; Parak, W. *Anal. Bioanal. Chem.* **2010**, *397*, 935−942.
(22) Qian, Z.; Bai, H.-J.; Wang, G.-L.; Xu, J.-J.; Chen, H.-Y. *Biosens. Bioelectron.* **2010**, *25*, 2045−2050.
(23) Zayats, M.; Willner, I., In *Biosensing for the 21st Century*; Renneberg, R., Lisdat, F., Eds.; Springer: Berlin, 2008; Vol. *109*, pp 255−283.
(24) Golub, E.; Niazov, A.; Freeman, R.; Zatsepin, M.; Willner, I. *J. Phys. Chem. C* **2012**, *116*, 13827−13834.
(25) Wang, J.; Liu, G.; Merkoçi, A. *J. Am. Chem. Soc.* **2003**, *125*, 3214−3215.
(26) de la Escosura-Muñiz, A.; Ambrosi, A.; Merkoçi, A. *Tr. Anal. Chem.* **2008**, *27*, 568−584.
(27) Wang, J.; Liu, G.; Wu, H.; Lin, Y. *Small* **2008**, *4*, 82−86.
(28) Cui, R.; Pan, H.-C.; Zhu, J.-J.; Chen, H.-Y. *Anal. Chem.* **2007**, *79*, 8494−8501.
(29) Willner, I.; Zayats, M. *Angew. Chem., Int. Ed.* **2007**, *46*, 6408−6418.
(30) Katz, E.; Willner, I.; Wang, J. *Electroanalysis* **2004**, *16*, 19−44.
(31) Chikkaveeraiah, B. V.; Bhirde, A. A.; Morgan, N. Y.; Eden, H. S.; Chen, X. *ACS Nano* **2012**, *6*, 6546−6561.
(32) Fang, X.; Han, M.; Lu, G.; Tu, W.; Dai, Z. *Sens. Actuators, B* **2012**, *168*, 271−276.
(33) Jiang, H.; Wang, X. *Anal. Chem.* **2012**, *84*, 6986−6993.
(34) Peng, S.; Zhang, X. *Microchim. Acta* **2012**, *178*, 323−330.
(35) Wang, H.; Chen, Q.; Tan, Z.; Yin, X.; Wang, L. *Electrochim. Acta* **2012**, *72*, 28−31.
(36) Wang, J.; Han, H.; Jiang, X.; Huang, L.; Chen, L.; Li, N. *Anal. Chem.* **2012**, *84*, 4893−4899.
(37) Jie, G.; Liu, B.; Pan, H.; Zhu, J.-J.; Chen, H.-Y. *Anal. Chem.* **2007**, *79*, 5574−5581.
(38) Sun, L.; Bao, L.; Hyun, B.-R.; Bartnik, A. C.; Zhong, Y.-W.; Reed, J. C.; Pang, D.-W.; Abruña, H. c. D.; Malliaras, G. G.; Wise, F. W. *Nano Lett.* **2008**, *9*, 789−793.
(39) Parak, W. J.; Hofmann, U. G.; Gaub, H. E.; Owicki, J. C. *Sens. Actuators, A* **1997**, *63*, 47−57.
(40) Owicki, J. C.; Wallace Parce, J. *Biosens. Bioelectron.* **1992**, *7*, 255−272.
(41) Yue, Z.; Khalid, W.; Zanella, M.; Abbasi, A.-Z.; Pfreundt, A.; Rivera Gil, P.; Schubert, K.; Lisdat, F.; Parak, W. J. *Analyt. Bioanalyt. Chem.* **2010**, *396*, 1095−1103.
(42) Xiao, F.; Lai, Y.; Zhang, N.; Bai, J.; Xian, Y.; Jin, L. *Chin. J. Chem.* **2012**, *30*, 1168−1176.
(43) Baş, D.; Boyacı, İ. *Analyt. Bioanalyt. Chem.* **2011**, *400*, 703−707.
(44) Bakkers, E.; Reitsma, E.; Kelly, J. J.; Vanmaekelbergh, D. *J. Phys. Chem. B* **1999**, *103*, 2781−2788.
(45) Bakkers, E.; Roest, A. L.; Marsman, A. W.; Jenneskens, L. W.; de Jong-van Steensel, L. I.; Kelly, J. J.; Vanmaekelbergh, D. *J. Phys. Chem. B* **2000**, *104*, 7266−7272.
(46) Hojeij, M.; Eugster, N.; Su, B.; Girault, H. H. *Langmuir* **2006**, *22*, 10652−10658.
(47) Hojeij, M.; Su, B.; Tan, S.; Mériguet, G.; Girault, H. H. *ACS Nano* **2008**, *2*, 984−992.
(48) Polymeropoulos, E. E. *J. Appl. Phys.* **1977**, *48*, 2404−2407.
(49) Su, B.; Fermín, D. J.; Abid, J.-P.; Eugster, N.; Girault, H. H. *J. Electroanal. Chem.* **2005**, *583*, 241−247.
(50) Bakkers, E.; Marsman, A. W.; Jenneskens, L. W.; Vanmaekelbergh, D. *Angew. Chem., Int. Ed.* **2000**, *39*, 2297−2299.
(51) Bakkers, E.; Kelly, J. J.; Vanmaekelbergh, D. *J. Electroanal. Chem.* **2000**, *482*, 48−55.
(52) Hickey, S. G.; Riley, D. J. *J. Phys. Chem. B* **1999**, *103*, 4599−4602.
(53) Hickey, S. G.; Riley, D. J. *Electrochim. Acta* **2000**, *45*, 3277−3282.
(54) Kuçur, E.; Bücking, W.; Nann, T. *Microchim. Acta* **2008**, *160*, 299−308.
(55) Eychmuller, A.; Hasselbarth, A.; Katsikas, L.; Weller, H. *Berichte Der Bunsen-Gesellschaft-Physical Chemistry Chemical Physics* **1991**, *95*, 79−84.
(56) Chestnoy, N.; Harris, T. D.; Hull, R.; Brus, L. E. *J. Phys. Chem.* **1986**, *90*, 3393−3399.
(57) Drouard, S.; Hickey, S. G.; Riley, D. J. *Chem. Commun.* **1999**, 67−68.
(58) Hickey, S. G.; Riley, D. J.; Tull, E. J. *J. Phys. Chem. B* **2000**, *104*, 7623−7626.
(59) Riley, D. J.; Tull, E. J. *J. Electroanal. Chem.* **2001**, *504*, 45−51.
(60) Peter, L. M.; Riley, D. J.; Tull, E. J.; Wijayantha, K. G. U. *Chem. Commun.* **2002**, 1030−1031.
(61) Riley, D. J.; Waggett, J. P.; Wijayantha, K. G. U. *J. Mater. Chem.* **2004**, *14*, 704−708.
(62) Doherty, R. P.; Hickey, S. G.; Riley, D. J.; Tull, E. J. *J. Electroanal. Chem.* **2004**, *569*, 271−274.

(63) Nakanishi, T.; Ohtani, B.; Uosaki, K. *J. Phys. Chem. B* **1998**, *102*, 1571−1577.
(64) Nakanishi, T.; Ohtani, B.; Shimazu, K.; Uosaki, K. *Chem. Phys. Lett.* **1997**, *278*, 233−237.
(65) Katz, E.; Zayats, M.; Willner, I.; Lisdat, F. *Chem. Commun.* **2006**, 1395−1397.
(66) Stoll, C.; Kudera, S.; Parak, W. J.; Lisdat, F. *Small* **2006**, *2*, 741−743.
(67) Schubert, K.; Khalid, W.; Yue, Z.; Parak, W. J.; Lisdat, F. *Langmuir* **2010**, *26*, 1395−1400.
(68) Yue, Z.; Zhang, W.; Wang, C.; Liu, G.; Niu, W. *Mater. Lett.* **2012**, *74*, 180−182.
(69) Stoll, C.; Gehring, C.; Schubert, K.; Zanella, M.; Parak, W. J.; Lisdat, F. *Biosens. Bioelectron.* **2008**, *24*, 260−265.
(70) Long, Y.-T.; Kong, C.; Li, D.-W.; Li, Y.; Chowdhury, S.; Tian, H. *Small* **2011**, *7*, 1624−1628.
(71) Baş, D.; Boyacı, İ. H. *Electroanalysis* **2009**, *21*, 1829−1834.
(72) Khalid, W.; El Helou, M.; Murböck, T.; Yue, Z.; Montenegro, J.-M.; Schubert, K.; Göbel, G.; Lisdat, F.; Witte, G.; Parak, W. J. *ACS Nano* **2011**, *5*, 9870−9876.
(73) Willner, I.; Patolsky, F.; Wasserman, J. *Angew. Chem., Int. Ed.* **2001**, *40*, 1861−1864.
(74) Yildiz, H. B.; Freeman, R.; Gill, R.; Willner, I. *Anal. Chem.* **2008**, *80*, 2811−2816.
(75) Golub, E.; Pelossof, G.; Freeman, R.; Zhang, H.; Willner, I. *Anal. Chem.* **2009**, *81*, 9291−9298.
(76) Khalid, W.; Göbel, G.; Hühn, D.; Montenegro, J. M.; Rivera-Gil, P.; Lisdat, F.; Parak, W. J. *J. Nanobiotechnol.* **2011**, *9*, 46.
(77) Poppe, J.; Gabriel, S.; Liebscher, L.; Hickey, S. G.; Eychmuller, A. *J. Mater. Chem. C* **2013**, *1*, 1515−1524.
(78) Ogawa, S.; Fan, F.-R. F.; Bard, A. J. *J. Phys. Chem.* **1995**, *99*, 11182−11189.
(79) Ogawa, S.; Hu, K.; Fan, F.-R. F.; Bard, A. J. *J. Phys. Chem. B* **1997**, *101*, 5707−5711.
(80) Hu, K.; Brust, M.; Bard, A. J. *Chem. Mater.* **1998**, *10*, 1160−1165.
(81) Kamat, P. V. *J. Phys. Chem. B* **2002**, *106*, 7729−7744.
(82) Kamat, P. V.; Shanghavi, B. *J. Phys. Chem. B* **1997**, *101*, 7675−7679.
(83) Sant, P. A.; Kamat, P. V. *Phys. Chem. Chem. Phys.* **2002**, *4*, 198−203.
(84) Sharma, S. N.; Pillai, Z. S.; Kamat, P. V. *J. Phys. Chem. B* **2003**, *107*, 10088−10093.
(85) Baker, D. R.; Kamat, P. V. *Adv. Funct. Mater.* **2009**, *19*, 805−811.
(86) Miyake, M.; Torimoto, T.; Nishizawa, M.; Sakata, T.; Mori, H.; Yoneyama, H. *Langmuir* **1999**, *15*, 2714−2718.
(87) Nakanishi, T.; Ohtani, B.; Uosaki, K. *Jpn. J. Appl. Phys.* **1997**, *36*, 4053−4056.
(88) Kamat, P. V. *J. Phys. Chem. C* **2008**, *112*, 18737−18753.
(89) Tang, J.; Sargent, E. H. *Adv. Mater.* **2011**, *23*, 12−29.
(90) Sargent, E. H. *Nat. Photonics* **2012**, *6*, 133−135.
(91) Sheeney-Haj-Ichia, L.; Wasserman, J.; Willner, I. *Adv. Mater.* **2002**, *14*, 1323−1326.
(92) Mann, S. *Nat. Mater.* **2009**, *8*, 781−792.
(93) Gowd, E. B.; Nandan, B.; Bigall, N. C.; Eychmüller, A.; Formanek, P.; Stamm, M. *Polymer* **2010**, *52*, 2661−2667.
(94) Gowd, E. B.; Nandan, B.; Vyas, M. K.; Bigall, N. C.; Eychmüller, A.; Schlörb, H.; Stamm, M. *Nanotechnology* **2009**, *20*, 415302.
(95) Nandan, B.; Gowd, E. B.; Bigall, N. C.; Eychmüller, A.; Formanek, P.; Simon, P.; Stamm, M. *Adv. Funct. Mater.* **2009**, *19*, 2805−2811.
(96) Miyake, M.; Matsumoto, H.; Nishizawa, M.; Sakata, T.; Mori, H.; Kuwabata, S.; Yoneyama, H. *Langmuir* **1997**, *13*, 742−746.
(97) Granot, E.; Patolsky, F.; Willner, I. *J. Phys. Chem. B* **2004**, *108*, 5875−5881.
(98) Etgar, L.; Moehl, T.; Gabriel, S.; Hickey, S. G.; Eychmuller, A.; Gratzel, M. *ACS Nano* **2012**, *6*, 3092−3099.
(99) Sheeney-Haj-Ichia, L.; Basnar, B.; Willner, I. *Angew. Chem., Int. Ed.* **2005**, *44*, 78−83.
(100) Sheeney-Haj-Ichia, L.; Pogorelova, S.; Gofer, Y.; Willner, I. *Adv. Funct. Mater.* **2004**, *14*, 416−424.
(101) Torimoto, T.; Nagakubo, S.; Nishizawa, M.; Yoneyama, H. *Langmuir* **1998**, *14*, 7077−7081.
(102) Göbel, G.; Schubert, K.; Schubart, I. W.; Khalid, W.; Parak, W. J.; Lisdat, F. *Electrochim. Acta* **2011**, *56*, 6397−6400.
(103) Zhao, W.-W.; Wang, J.; Xu, J.-J.; Chen, H.-Y. *Chem. Commun.* **2011**, *47*, 10990−10992.
(104) Zhao, W.-W.; Yu, P.-P.; Shan, Y.; Wang, J.; Xu, J.-J.; Chen, H.-Y. *Anal. Chem.* **2012**, *84*, 5892−5897.
(105) Robel, I.; Bunker, B. A.; Kamat, P. V. *Adv. Mater.* **2005**, *17*, 2458−2463.
(106) Tu, W.; Wang, W.; Lei, J.; Deng, S.; Ju, H. *Chem. Commun.* **2012**, *48*, 6535−6537.
(107) Brown, P.; Kamat, P. V. *J. Am. Chem. Soc.* **2008**, *130*, 8890−8891.
(108) Nasr, C.; Kamat, P. V.; Hotchandani, S. *J. Electroanal. Chem.* **1997**, *420*, 201−207.
(109) Robel, I.; Subramanian, V.; Kuno, M.; Kamat, P. V. *J. Am. Chem. Soc.* **2006**, *128*, 2385−2393.
(110) Wang, G.-L.; Xu, J.-J.; Chen, H.-Y.; Fu, S.-Z. *Biosens. Bioelectron.* **2009**, *25*, 791−796.
(111) Yildiz, H. B.; Tel-Vered, R.; Willner, I. *Adv. Funct. Mater.* **2008**, *18*, 3497−3505.
(112) Shen, Q.; Zhao, X.; Zhou, S.; Hou, W.; Zhu, J.-J. *J. Phys. Chem. C* **2011**, *115*, 17958−17964.
(113) Yildiz, H. B.; Tel-Vered, R.; Willner, I. *Angew. Chem., Int. Ed.* **2008**, *47*, 6629−6633.
(114) Tel-Vered, R.; Yildiz, H. B.; Willner, I. *Adv. Mater.* **2009**, *21*, 716−720.
(115) Ovits, O.; Tel-Vered, R.; Baravik, I.; Wilner, O. I.; Willner, I. *J. Mater. Chem.* **2009**, *19*, 7650−7655.
(116) Guo, C. X.; Yang, H. B.; Sheng, Z. M.; Lu, Z. S.; Song, Q. L.; Li, C. M. *Angew. Chem., Int. Ed.* **2010**, *49*, 3014−3017.
(117) Zhang, X.; Li, S.; Jin, X.; Zhang, S. *Chem. Commun.* **2011**, *47*, 4929−4931.
(118) Wang, G.-L.; Yu, P.-P.; Xu, J.-J.; Chen, H.-Y. *J. Phys. Chem. C* **2009**, *113*, 11142−11148.
(119) Baron, R.; Huang, C.-H.; Bassani, D. M.; Onopriyenko, A.; Zayats, M.; Willner, I. *Angew. Chem., Int. Ed.* **2005**, *44*, 4010−4015.
(120) Xu, J.-P.; Weizmann, Y.; Krikhely, N.; Baron, R.; Willner, I. *Small* **2006**, *2*, 1178−1182.
(121) Tel-Vered, R.; Yehezkeli, O.; Yildiz, H. B.; Wilner, O. I.; Willner, I. *Angew. Chem., Int. Ed.* **2008**, *47*, 8272−8276.
(122) Freeman, R.; Gill, R.; Beissenhirtz, M.; Willner, I. *Photochem. Photobiol. Sci.* **2007**, *6*, 416−422.
(123) Gill, R.; Patolsky, F.; Katz, E.; Willner, I. *Angew. Chem., Int. Ed.* **2005**, *44*, 4554−4557.
(124) Pardo-Yissar, V.; Katz, E.; Wasserman, J.; Willner, I. *J. Am. Chem. Soc.* **2003**, *125*, 622−623.
(125) Tanne, J.; Schäfer, D.; Khalid, W.; Parak, W. J.; Lisdat, F. *Anal. Chem.* **2011**, *83*, 7778−7785.
(126) Tang, L.; Zhu, Y.; Yang, X.; Sun, J.; Li, C. *Biosens. Bioelectron.* **2008**, *24*, 319−323.
(127) Wang, G.-L.; Xu, J.-J.; Chen, H.-Y. *Nanoscale* **2010**, *2*, 1112−1114.
(128) Zheng, M.; Cui, Y.; Li, X.; Liu, S.; Tang, Z. *J. Electroanal. Chem.* **2011**, *656*, 167−173.
(129) Riedel, M.; Göbel, G.; Abdelmonem, A. M.; Parak, W. J.; Lisdat, F. *Chemphyschem* **2013**, DOI: 10.1002/cphc.201201036.
(130) Zhao, W.-W.; Yu, P.-P.; Xu, J.-J.; Chen, H.-Y. *Electrochem. Commun.* **2011**, *13*, 495−497.
(131) Zhao, W.-W.; Ma, Z.-Y.; Yu, P.-P.; Dong, X.-Y.; Xu, J.-J.; Chen, H.-Y. *Anal. Chem.* **2012**, *84*, 917−923.
(132) Chen, D.; Zhang, H.; Li, X.; Li, J. H. *Anal. Chem.* **2010**, *82*, 2253−2261.

(133) Yang, X.; Wang, P.; Zhu, Y.; Li, C. *J. Solid State Electrochem.* **2011**, *15*, 731−736.
(134) Curri, M. L.; Agostiano, A.; Leo, G.; Mallardi, A.; Cosma, P.; Della Monica, M. *Mater. Sci. Eng., C* **2002**, *22*, 449−452.
(135) Vastarella, W.; Nicastri, R. *Talanta* **2005**, *66*, 627−633.
(136) Zhang, X.; Li, S.; Jin, X.; Li, X. *Biosens. Bioelectron.* **2011**, *26*, 3674−3678.